Semi-Annual Report

NASA NAG-1-394

Fundamental Studies of Structure Borne Noise for Advanced Turboprop Applications

(NASA-CR-175737) FUNDAMENTAL STUDIES OF STRUCTURE BORNE NOISE FOR ADVANCED TURBOPROP APPLICATIONS Semiannual Report (Missouri Univ.) 14 p HC A02/MF A01 CSCL 20A
N85-26320
Unclas
G3/71 21144

W. Eversman

L. R. Koval

Department of Mechanical and Aerospace Engineering

University of Missouri-Rolla

Rolla, Missouri 65401

May 1985

Introduction

The purpose of this interim report is to outline the methods being employed to meet the objectives of NASA Grant NAG-1-394 "Fundamental Studies of Structure Borne Noise for Advanced Turboprop Applications." The problem considered is the transmission of sound generated by wing mounted advanced turboprop engines into the cabin interior via structural paths and the comparison of the interior noise level due to the airborne and structure borne components. The goal is the assessment of the relative importance of the two sources of interior noise.

The structural model employed is a beam representation of the wing box carried into the fuselage via a representative frame type of carry through structure. The structure for the cabin cavity is a stiffened shell of rectangular or cylindrical geometry. The structure is modelled using a finite element formulation and the acoustic cavity is modelled using an analytical representation appropriate for the geometry. The structural and acoustic models are coupled by the use of hard wall cavity modes for the interior and vacuum structural modes for the shell. The coupling method is similar to that employed by Craggs and Lau [1] and Dowell, Gorman, and Smith [2]. In the present study the coupling is accomplished using a combination of analytical and finite element models. The advantage is the substantial reduction in dimensionality achieved by modelling the interior analytically.

Mathematical Model

The mathematical model for the interior noise problem is readily demonstrated here with a simple plate/cavity system which has all of the features of the fuselage interior noise problem. The final model will replace the structural representation with a stiffened shell and wing. The final model for the cavity is no more detailed than described here, except that a cylindrical geometry can be used.

A. Cavity Model

The cavity is here modelled as rectangular with dimensions a, b, c. The face a,b is the plate, as shown in Figure 1. The acoustic environment within the cavity is governed by the field equations and boundary conditions

$$\nabla^2 p = \frac{1}{c_0^2} p_{tt} \qquad (1)$$

$$\frac{\partial p}{\partial n} = 0 \quad \text{on} \quad C \qquad (2)$$

$$\frac{\partial p}{\partial n} = -\rho_0 w_{tt} \quad \text{on} \quad S \qquad (3)$$

where p is the acoustic pressure, n is the outward normal at the cavity walls, ρ_0 and c_0 are the ambient density and speed of sound in the air within the cavity, C is the portion of the cavity boundary which is rigid and S is the boundary of the cavity which is structural (the plate in the present case). w is the displacement of the structure at the fluid/structure interface, positive when directed outward. It is seen that the cavity acoustic pressure is driven by the acceleration of the structural walls.

A weak formulation of the acoustic problem is written as

$$\iiint_{V} W_i[\nabla^2\hat{p} - \frac{1}{c_0^2}\hat{p}_{tt}]dV - \iint_{S} W_i[\frac{\partial\hat{p}}{\partial n} + \rho_0 w_{tt}]dA - \iint_{C} W_i \frac{\partial\hat{p}}{\partial n}\, dA = 0 \tag{4}$$

where the sum of the volume weighted residual of the field equation for a trial solution $\hat{p}$ from the class of continuous functions and the surface-weighted boundary residuals vanish for all weighting functions W_i from the class of continuous functions. If the weighting functions are constructed from the complete orthogonal set defined by solutions of

$$\nabla^2 W + \frac{\Omega^2}{c_0^2} W = 0 \tag{5}$$

$$\nabla W \cdot \vec{n} = 0 \quad \text{on} \quad C \text{ and } S$$

then the weak formulation can be written, after two applications of the divergence theorem, as

$$\iiint_{V} W_i\,[\hat{p}_{tt} + \Omega^2\hat{p}]dV + \iint_{S} \rho_0 c_0^2 W_i w_{tt} dA = 0 \tag{6}$$

Next, the trial solution is constructed from the same complete orthogonal set defined by equation (5)

$$\hat{p} = \sum A_i W_i(x,y,z) = [W(x,y,z)]\,\{A\} \tag{7}$$

where [W(x,y,z)] is a row vector of acoustic hardwall mode shapes. Equation (6) now becomes

$$\iiint_{V}([W]^T[W]\,\{A_{tt}\} + [\ \Omega^2\ ][W]^T[W]\{A\})dV$$

$$+ \rho_0 c_0^2 \iint_S [W]^T w_{tt} dA = 0 \tag{8}$$

By virtue of the orthogonality properties of the acoustic hardwall mode shapes defined by equation (5) it is found that

$$\iiint_{\forall} [W]^T [W] d\forall = [\ulcorner N_{nn} \lrcorner] \tag{9}$$

where $[\ulcorner N_{nn} \lrcorner]$ is a diagonal matrix of "acoustic generalized masses." Equation (8) becomes

$$[\ulcorner N_{nn} \lrcorner]\{A_{tt}\} + [\ulcorner \Omega^2 \lrcorner][\ulcorner N_{nn} \lrcorner]\{A\} = -\rho_0 c_0^2 \iint_S [W]^T w_{tt} dA \tag{10}$$

Equation (10) yields the unknown amplitude coefficients in the acoustic pressure representation of equation (7) for specified structural wall acceleration w_{tt}. For the rectangular cavity discussed here the acoustic hardwall modes are

$$W_i = W_{\ell mn} = \cos \ell\pi \frac{x}{a} \cos m\pi \frac{y}{b} \cos m\pi \frac{z}{c} \tag{11}$$

B. Structural Model

The structural model discussed here is a simple uniform plate of dimension a,b. The dynamics of the plate are described by the familiar result

$$D \nabla^4 w + \rho h \, w_{tt} = -(p_a - p) \tag{12}$$

where

$$D = \frac{Eh^3}{12(1-\nu^2)}$$

E = Young's modulus

h = plate thickness

ν = Poisson's Ratio

ρ = plate mass density

The applied pressure loading is p_a and the pressure loading due to the cavity is p. The sign convention is set up so that the positive plate displacement is out of the cavity, consistent with the cavity model. Boundary conditions on the plate can be specified as desired. For fuselage modelling the plate or shell model would have built in edges. For the present discussion, where it is convenient to speak in terms of an analytical representation of the mode shapes, it is simpler to use a simply supported condition.

A weighted residuals formulation for the plate can be written

$$\iint_S \psi_i \, [D \nabla^4 w + \rho h \, w_{tt} + p_a - p] dA = 0 \tag{13}$$

This becomes a classical Galerkin formulation if we choose the weighting functions ψ_i to be solutions of

$$D \nabla^4 \psi_i - \rho h \omega_i^2 \psi_i = 0 \tag{14}$$

with the same boundary conditions as the plate and also expand the solution w in terms of these functions

$$w(x,y) = \sum q_n \psi_n(x,y) = [\psi]\{q\} \tag{15}$$

where $[\psi]$ is a row matrix of eigenfunctions.

If a finite element formulation is used the expansion is given by

$$w(x,y) = [N][\Psi]\{q\} \tag{16}$$

where [N] is a global shape function matrix (interpolation matrix) and $[\Psi]$ is the model matrix (matrix with eigenvectors as columns) determined from a finite element solution of equation (14). The interpolation matrix is not explicitly defined globally, but consistent with finite element methods is defined on subdomains (elements). In the case of the plate the shape functions have continuous first derivatives. Equation (13) is written in terms of the unknown modal amplitudes as

$$\iint_S \rho h([\Psi]^T[\Psi]\{q_{tt}\} + [\nwarrow \omega^2 \searrow][\Psi]^T[\Psi]\{q\})dA$$
$$= \iint [\Psi]^T p dA - \iint [\Psi]^T p_a dA \tag{17}$$

The plate modes are orthogonal according to

$$\iint_S \rho h[\Psi]^T[\Psi]dA = [\nwarrow M_{nn} \searrow] \tag{18}$$

Equation (17) now becomes

$$\lceil M_{nn} \rfloor \{q_{tt}\} + \lceil \omega^2 \rfloor \lceil M_{nn} \rfloor \{q\} = \iint [\Psi]^T p dA - \iint [\Psi]^T p_a dA \qquad (19)$$

When finite element methods are used to obtain the mode shapes, equation (19) is written

$$\lceil M_{nn} \rfloor \{q_{tt}\} + \lceil \omega^2 \rfloor \lceil M_{nn} \rfloor \{q\} = [\Psi]^T \iint [N]^T p dA - [\Psi]^T \iint [N]^T p_a dA \qquad (20)$$

The coupled plate and cavity equations are now (10) and (20)

$$\begin{aligned} &\lceil M_{nn} \rfloor \{q_{tt}\} + \lceil \omega^2 \rfloor \lceil M_{nn} \rfloor \{q\} - [\Psi]^T \iint_S [N]^T p dA = [\Psi]^T \iint_S [N]^T p_a dA \\ &\lceil N_{nn} \rfloor \{A_{tt}\} + \lceil \Omega^2 \rfloor \lceil N_{nn} \rfloor \{A\} + \rho_0 c_0^2 \iint_S [W]^T w_{tt} dA = 0 \end{aligned} \qquad (21)$$

The integrals $[\Psi]^T \iint_S [N]^T p dA$ and $\rho_0 c_0^2 \iint_S [W]^T w_{tt} dA$ are coupling matrices which can be rewritten using equations (7) and (16)

$$[\Psi]^T \iint_S [N]^T p dA = [\Psi]^T \iint_S [N]^T [W] dA \{A\} \qquad (22)$$

$$\rho_0 c_0^2 \iint_S [W]^T w_{tt} dA = \rho_0 c_0^2 \iint_S [W]^T [N] dA [\Psi] \{q_{tt}\} \qquad (23)$$

If we introduce the definition

$$[\theta] = [\Psi]^T \iint_S [N]^T [W] dA$$

then equations (21) can be written

$$\lceil M_{nn} \rfloor \{q_{tt}\} + \lceil \omega^2 \rfloor \lceil M_{nn} \rfloor \{q\} - [\theta]\{A\} = [F]\{p\} \qquad (24)$$

$$\lceil N_{nn} \rfloor \{A_{tt}\} + \lceil \omega^2 \rfloor \lceil N_{nn} \rfloor \{A\} + \rho_0 c_0^2 [\theta]^T \{q_{tt}\} = 0 \qquad (25)$$

where we have interpolated p_a according to

$$p_a = [N]\{p_a\}$$

with $\{p_a\}$ being nodal values of p_a (and derivatives if required) and

$$[F] = [\Psi]^T \iint_S [N]^T[N]dA \tag{26}$$

Equations (22) and (23) show that the coupling matrices are related to transposes of one another. The integrals in equations (22) and (23) and the integral defining [F] in equation (26) can be evaluated by usual finite element techniques of integration over subdomains (elements) using shape functions which are explicitly defined on the subdomain.

In the case of the plate, the shape functions are Hermitian polynomials which in the rectangular plate geometry load to conforming elements with complete slope continuity at element boundaries. In a completely consistent formulation of the integrals in equations (22), (23), and (26) the shape functions implied by the global shape matrix [N] should be Hermitian as required by the finite element analysis of equation (14) which leads to the modal expansion of equation (16). The finite element analysis of equation (14) to obtain the modal matrix $[\Psi]$ certainly requires slope continuity in the shape functions. The coupling matrix $[\theta]$ does not require this much continuity and an interpolation based on only the nodal values of the weighting functions and the pressure or plate displacements is satisfactory. Hence, the most versatile procedure would evaluate the coupling matrix $[\theta]$ and input generalized force distribution matrix [F] with the element shape matrices representing quadratic interpolation on 8 or 9 noded isoparametric elements. The modal matrix $[\Psi]$ is compressed to include only the displacement degrees of freedom. This procedure results in no detectable compromise in accuracy and allows experimentation with element types for the plate (or shell) model without requiring a reformulation of the coupling matrix computation.

Equations (24) and (25) represent a set of coupled second order ordinary differential equations with generalized coordinates representing the plate modal amplitudes and the acoustic cavity modal amplitudes. Dissipation is not explicitly included in these equations but can easily be included as structural damping in the plate generalized stiffness matrix or as an equivalent viscous damping. Dissipative walls in the cavity can also be modelled.

Equations (24) and (25) can be written in the form of a general dynamic system

$$[M]\{\ddot{x}\} + [C]\{\dot{x}\} + [K]\{x\} = \{Q\} \tag{27}$$

where the generalized coordinates {x} are the vectors {q} and {A} and the matrices [M] and [K] can be constructed from equations (24) and (25). The viscous damping matrix can be constructed from equivalent damping for the structure or for dissipative walls. The generalized force vector {Q} is also easily identifiable in equations (24) and (25).

The model for a stiffened fuselage structure is more complicated only in the structural modelling. All steps taken here will apply, however the finite element model for the structural mode shapes will be more complicated.

Solution Methods

It is presumed that the acoustic input to the structure is given in terms of its Fourier spectrum. That is

$$Q(\omega) = \int_{-\infty}^{\infty} Q(t)\ e^{-i\omega t}dt \tag{28}$$

where $Q(\omega)$ is the Fourier spectrum in

$$Q(t) = \frac{1}{2\pi}\int_{-\infty}^{\infty} Q(\omega)\ e^{i\omega t}d\omega \tag{29}$$

Fourier Transform methods lead to the solution for the Fourier Spectra of the output generalized coordinates

$$\{X(\omega)\} = [D(\omega)]^{-1}\{Q(\omega)\} \tag{30}$$

where $[D(\omega)]$ is defined by

$$[D(\omega)] = [K] - \omega^2[M] + i\omega[C] \tag{31}$$

The acoustic pressure at any point within the cavity can be obtained from the acoustical modal amplitudes contained in $\{X(\omega)\}$. Write

$$\{A(\omega)\} = [T_a(\omega)]\{Q(\omega)\} \tag{32}$$

where $[T_a(\omega)]$ is the acoustic transfer function which is obtained by deleting rows from $[D(\omega)]^{-1}$ corresponding to the plate degrees of freedom. The acoustic pressure is obtained from

$$\begin{aligned} P(x,y,z,\omega) &= [W(x,y,z)]\{A(\omega)\} \\ &= [W(x,y,z)][T_a(\omega)]\{Q(\omega)\} \end{aligned} \tag{33}$$

The energy density spectrum for the acoustic response at a point in the cavity is determined from the definition of the autocorrelation

$$\phi(\tau) = \int_{-\infty}^{\infty} P(t)p(t + \tau)d\tau$$

and its Fourier Transform

$$\Phi(\omega) = \int_{-\infty}^{\infty} \phi(\tau)e^{-i\omega\tau}d\tau = |P(\omega)|^2$$

The inverse relationship

$$\phi(\tau) = \frac{1}{2\pi} \int_{-\infty}^{\infty} |P(\omega)|^2 e^{i\omega\tau}d\omega$$

leads to the conclusion

$$\phi(0) = \int_{-\infty}^{\infty} p^2(t)dt = \frac{1}{2\pi} \int_{-\infty}^{\infty} |P(\omega)|^2 d\omega = \int_{-\infty}^{\infty} |P(f)|^2 df$$

This identifies the energy density spectrum $|P(f)|^2$ as a measure of the system response since the "total energy" $\int_{-\infty}^{\infty} p^2(t)dt$ is given by an integral over all frequencies of the energy density. From equation (33)

$$|P(\omega)|^2 = \{Q^*(\omega)\}^T[T_a^*(\omega)]^T[W]^T[W][T_a(\omega)]\{Q(\omega)\}$$

where the star represents the complex conjugate. The volume average of this is

$$|\overline{P(\omega)}|^2 = \{Q^*(\omega)\}^T[T_a^*(\omega)]^T[\ N_{nn}\ ][T_a(\omega)]\{Q(\omega)\}$$

where $[\ N_{nn}\ ]$ is defined by equation (9). Hence we write

$$|\overline{P(\omega)}|^2 = \{A^*(\omega)\}^T[\ N_{nn}\ ]\{A(\omega)\}$$

$$= \sum N_{nn}\ |A_n(\omega)|^2 \tag{34}$$

A suitable measure of the cavity response is thus the weighted sum of the absolute values squared of the acoustic modal amplitudes. A suitable normalization of the cavity modes could be used to make the weighting factors N_{nn} unity.

Results

The major effort to date has been expended in verification of the computer implementation. The following tasks have been undertaken:

(1) Evaluation of plate elements with emphasis on convergence to exact free vibration mode shapes. This has established the Hermitian element as superior.

(2) Evaluation of shell elements, again with emphasis on free vibration convergence. The 32 degrees of freedom extension of the Bogner-Schmidt plate element produces the best results in the present case.

(3) Detailed comparisons of fully analytic and combination finite element/analytic modes for the rectangular cavity - plate system. These comparisons were performed to verify the essential features of the coding relating to the coupling of the plate and cavity. Figure 2 shows a response spectrum for a plate-cavity system generated from a finite element plate model and analytic cavity model. Comparison with computations of Craggs and Lau is good. Comparison with a fully analytic modal representation for both plate and cavity is excellent. The results for the fully analytic model is shown on a different scale in Figure 3.

(4) Substantial progress has been made in the finite element modelling of stiffened plates and shells. These will be coupled with the analytic cavity models in the near future.

Effort will be started to couple the wing to the plate and shell models and to synthesize a reasonable model for propeller interaction with the wing as a noise source model. An available propeller noise prediction program will be used to derive an equivalent airborne noise field for the purposes of comparing the airborne and structure borne interior noise.

References

1. A. Craggs and M. G. Lau, Institute of Sound and Vibration Research Report, "Recent Advances in Structural Dynamics, Volume 2." Edited by M. Petyt, 437-445. Finite Element Applications to Coupled Plate-Acoustic Absorption Systems.

2. E. H. Dowell, G. F. Gorman, and D. A. Smith 1977 Journal of Sound and Vibration 52(4), 519-542. Acoustoelasticity: General Theory, Acoustic Natural Modes and Forced Response to Sinusoidal Excitation, Including Comparisons with Experiment.

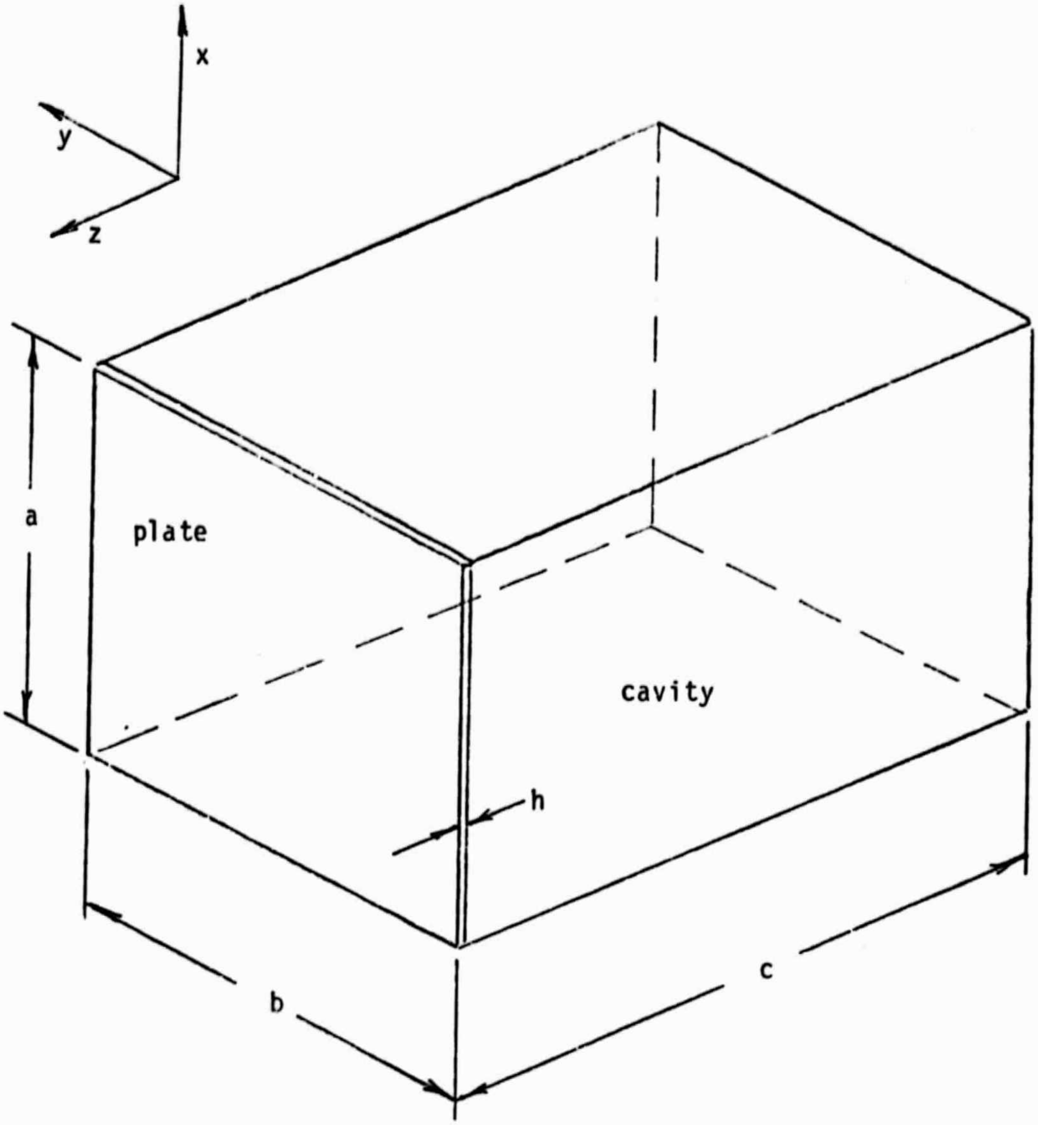

Figure 1. Plate Cavity System.

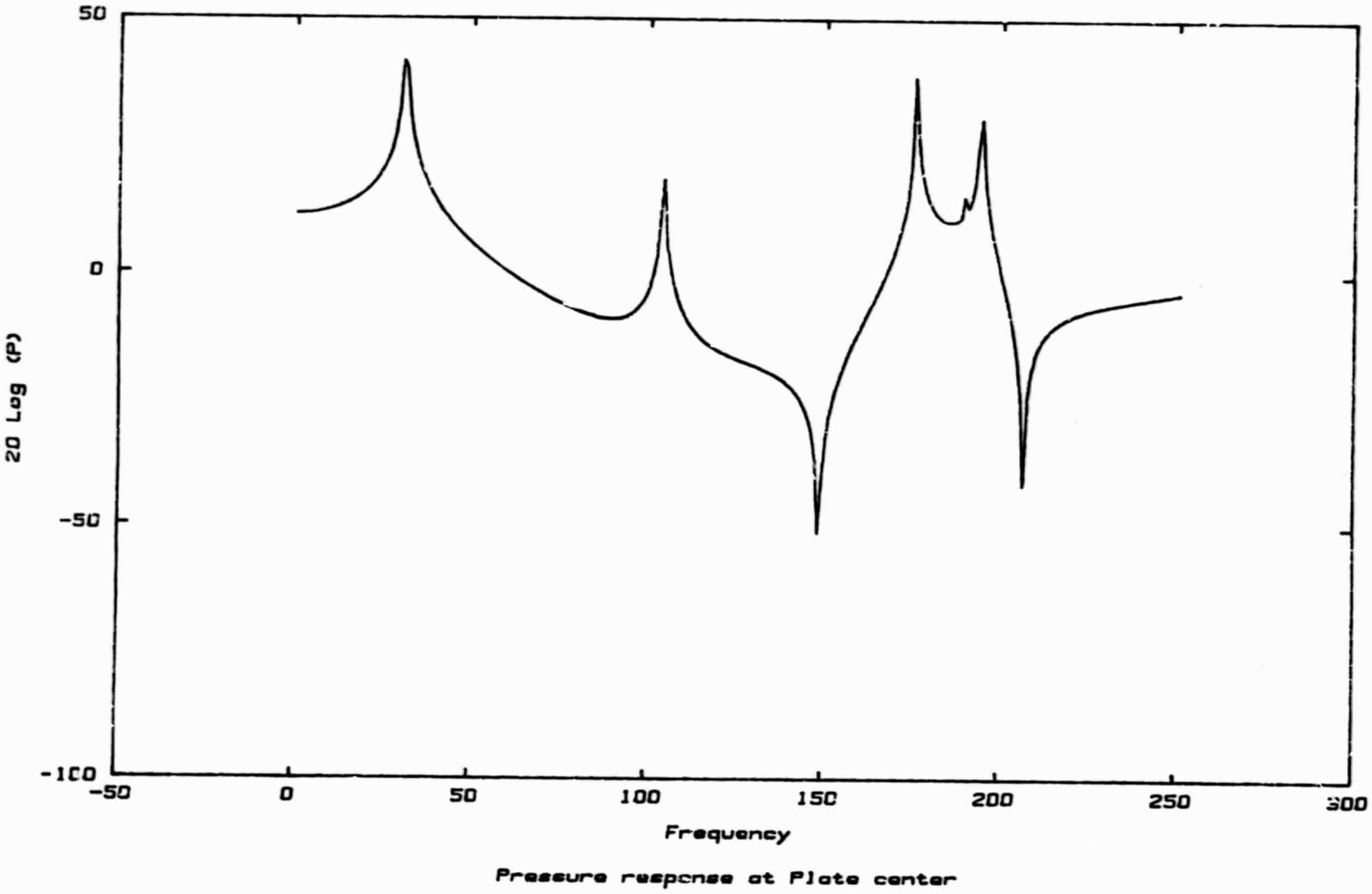

Figure 2. Example of a Coupled Plate-Cavity Transfer Function.

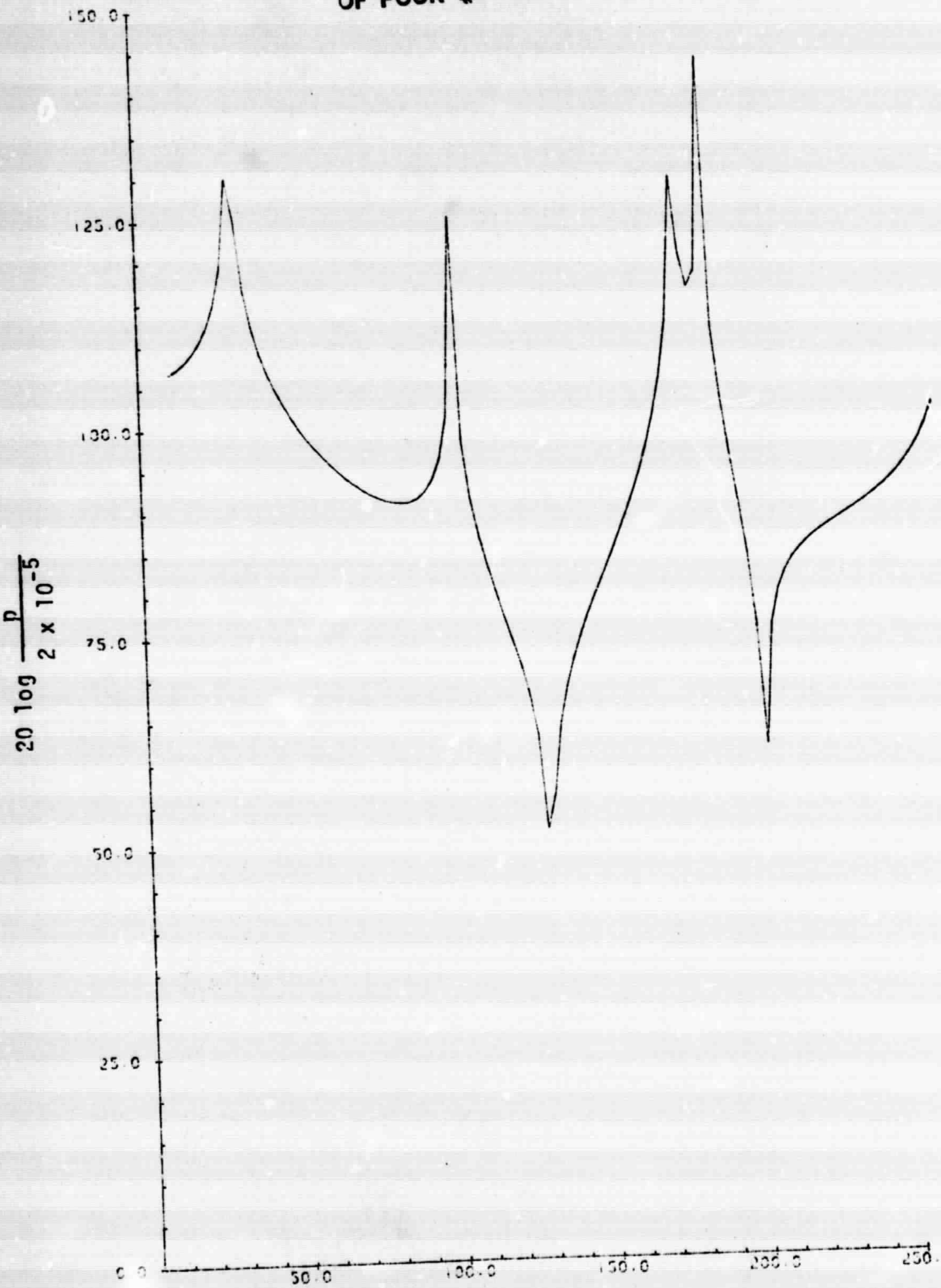

Figure 3. Frequency response using analytic plate modes and cavity modes.